

RESEARCH ARTICLE

A Millimeter-Wave Six-Port Junction Based on Ridge Gap Waveguide

DAVOUD ZARIFI¹, ALI FARAHBAKHS²,
AND ASHRAF UZ ZAMAN³, (Senior Member, IEEE)

¹School of Electrical and Computer Engineering, University of Kashan, Kashan 87317-53153, Iran

²Department of Electrical and Computer Engineering, Graduate University of Advanced Technology, Kerman 76311-33131, Iran

³Department of Electrical Engineering, Chalmers University of Technology, 412 96 Göteborg, Sweden

Corresponding author: Davoud Zarifi (zarifi@kashanu.ac.ir)

ABSTRACT The current paper presents a six-port low-loss waveguide coupler based on ridge gap waveguide structure with potential application in various mmWave wireless systems. The challenges in the fabrication faced in mmWave frequencies can be overcome by using the gap waveguide technology. The excitation of presented six-port junction is done by standard WR-28 waveguide flanges at the bottom. The performance of the proposed structure is confirmed by the fabrication and measurement. The measured results show that the proposed six-port junction operates in 30 GHz with 15% bandwidth with return loss in both input ports and isolation level better than 15 dB and 15 dB, respectively. The findings are valuable for the design and development of mmWave junctions for use in various high-frequency applications.

INDEX TERMS Six-port junction, gap waveguide technology, mmWave.

I. INTRODUCTION

The attention of the research community to the mmWave frequency band has recently been increased because it has functional advantages for many applications. With the help of novel technology development at this frequency band, various wireless applications such as high-speed internet, high-definition video streaming, high-definition multimedia interface, automotive radars, and wireless gigabit Ethernet will be made possible. [1]. However, the robustness of passive RF components and easy integration with other wireless system's components are important factors affecting the performance and reduction of the system cost at mmWave frequency range.

Six-port junctions are the key components of various mmWave networks for different microwave applications such as reflection measurements, direct receiver systems, power detecting systems, vibration measurement, calibration of automotive radars, displacement detection and mechanical stress diagnosis [2], [3], [4]. A six-port junction is made up of dividers and combiners that are linked together to create

four separate sums of a reference signal and the signal to be measured. In this junction, the two input signals are combined in four different phase configurations at the four outputs. Six-port junctions were first introduced as alternatives for vector network analysis and in power-measuring devices and then have been extended to replace conventional mixers in homodyne and heterodyne receivers. For the measurement purposes, one of the six ports of the junction is connected to a source as an input port and another is connected to an unknown load. The reflection coefficient of the unknown load can be determined by measuring the power appearing in on the other four ports. In a direct receiver system, local oscillator and RF signal are considered as input ports of six-port junction and I/Q signals of quadrature phase are as the four output ports.

Good impedance matching, low insertion loss and wide-band transfer characteristics are the desired design objectives for such a six-port junction or coupler. The six-port junctions can be designed and implemented in three types of architecture: three 3-dB directional couplers along a 1-to-2 way power splitter [2]; four 3-dB directional couplers along a phase shifter [5]; and two 3-dB directional couplers along two power dividers and a 90° phase shifter [6]. In the first

The associate editor coordinating the review of this manuscript and approving it for publication was Photos Vryonides¹.

type of architecture, six-port junctions with simple structures, wide bandwidth and high isolation between the inputs and outputs ports can be achieved as it does not need extra phase-shifters.

Researchers have proposed various types of six-port junctions including microstrip, substrate integrated waveguide (SIW) and rectangular waveguide based structures. Microstrip- and SIW-based six-port junctions are light-weighted and compact, and their production is relatively low cost [6], [7], [8], [9], [10], [11], [12]. Moreover, their integration with other active and passive mmWave components in the wireless system is easy. Nevertheless, there are some drawbacks in these structures, such as high dielectric and ohmic losses and leakage as surface waves at high frequency. Rectangular waveguide structures are low loss and can handle high power levels, but high precision, accurate, and costly manufacturing and difficult integration limit their usage in mmWave applications [13], [14], [15], [16], [17], [18]. Particularly, providing acceptable electrical contact between the structure's various metal layers in the rectangular waveguide structures is a serious challenge in mmWave frequencies. In addition, these structures are difficult to be integrated with RF circuits. Therefore, there is a need to use another technology than rectangular waveguides and PCB-based technologies.

In recent years, gap waveguide technology has been developed to overcome the difficulty of fabrication of various microwave components at mmWave frequency range [19]. In mmWave frequencies, the gap waveguide technology is employed to eliminate fabrication related problems of slot array antennas [20], [21], [22], couplers and dividers [23], [24], [25], magic-T [26], mechanical switches [27] and printed gap waveguide-based six-port junction [28]. All these components show promising performance at mmWave frequency range. Also, gap waveguide has been demonstrated with very good packaging and RF electronics integration feature at mmWave range [29], [30], in this work, we present the design and fabrication of a broadband ridge gap waveguide-based six-port junction which has simple geometry, wideband and low-loss performance. The main novelty of the work presented in this paper is based on proposing ridge gap waveguide-based six-port junction in order to overcome the difficulty of fabrication at mmWave frequency. To the authors' knowledge, design of ridge gap waveguide-based six-port coupler for mmWave applications is discussed for the very first time. By employing gap waveguide technology and providing acceptable electrical contact between the layers, the manufacturing and assembly process will be simple and non-expensive. The measurement results demonstrate that the reflection coefficients of input ports of the proposed structure are is than -15 dB with the isolation higher than 15 dB over the frequency range of 27.7-32.2 GHz.

The ridge gap waveguide structure and its stop-band are described in Section II. Sections III is devoted to the simulation and design of the proposed ridge gap waveguide-based six-port junction. The details of the fabricated prototype

and the measurements presented in Section IV and some conclusions are drawn in Section V.

II. RIDGE GAP WAVEGUIDE STRUCTURE

Gap waveguide technology is used to overcome the difficulty of maintaining perfect electrical contact among the waveguide blocks by using perfect magnetic conductor (PMC) wall which is implemented by periodic metal pins and air gap Fig. 1(a). Generally, the ridge gap waveguide structures are more compact than groove gap waveguides. Planar metal surfaces with small periodic metal texture in the form of rectangular pins can be easily produced using various well established manufacturing technologies such as CNC milling. In the gap waveguide structures, ridges and grooves are employed as guiding structures to control the propagation direction of the electromagnetic waves. Within the parallel plate stop-band of the periodic structure, periodic pins around the guiding lines can prevent waves to propagate in undesired directions. To achieve the required performance over the desired frequency bandwidth, the dimensions of the pins (material: Aluminum), their periodicity, the air gap and width of ridge should be carefully chosen [19]. With the help of CST Microwave Studio and its eigen-mode solver, the geometrical parameters have been design and following dimensions $a = 1$ mm, $d = 3$ mm, $g = 0.5$ mm, and $p = 1$ mm have been chosen to form a stop-band from 22 to 38 GHz and this is demonstrated in Fig. 1(b).

III. DESIGN OF SIX-PORT JUNCTION

A. RIDGE GAP WAVEGUIDE-BASED 3-DB COUPLER

Topology of the ridge gap waveguide-based 3-dB coupler is shown in Fig. 2. Significant improvement in bandwidth can be achieved by using a multi-section design. To achieve constant coupling, low input reflection coefficient and higher isolation over a wide bandwidth, a multiple-section branch-line coupler is employed here. The lengths and widths of the shunt and series branches should be adjusted to achieve the desired power splitting ratio. The optimization problem is solved by applying a computer-aided design that limits the minimum and maximum allowable values for ridge width and pin periodicity.

To achieve desired S-parameters, the values of the geometrical parameters of the structure should be optimized. Optimization based on Trust Region Framework in CST Microwave Studio find the optimized values of structure geometrical parameters assuming an appropriate fitness function which is defined as:

$$Fitness = \left(\frac{1}{M} \sum_{m=1}^M \left(|S_{11}(f_m)|^2 + |S_{21}(f_m) - 3|^2 + |S_{31}(f_m) - 3|^2 + |S_{41}(f_m)|^2 \right) \right)^{0.5} \quad (1)$$

The simulated S-parameters of the 3-dB directional coupler are plotted in Fig. 3. Observe that the return loss is better than 18 dB, and the insertion loss in the coupled branches

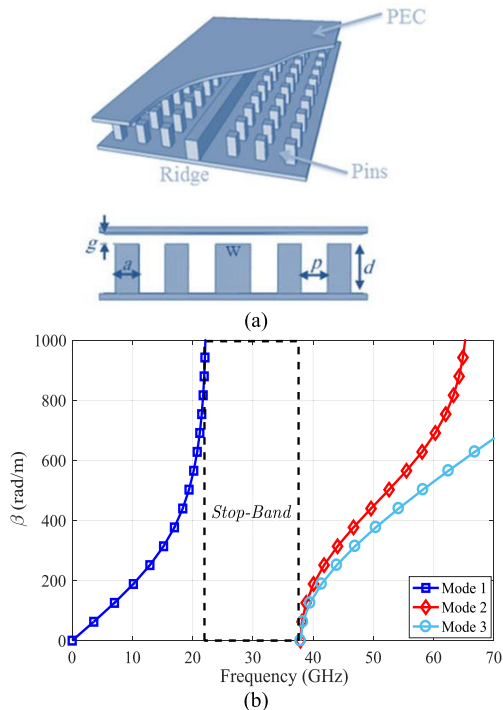


FIGURE 1. (a) Ridge gap waveguide structure. (b) Dispersion diagram of the periodic metallic pins.

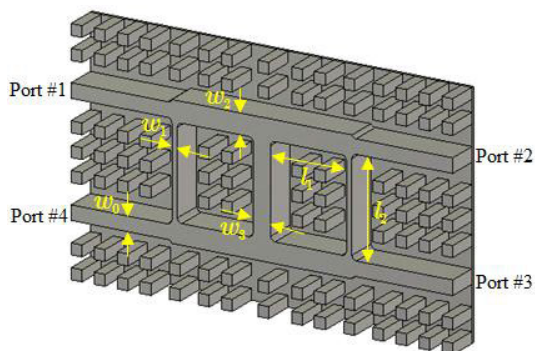


FIGURE 2. The configuration of ridge gap waveguide-based 3-dB directional coupler without top metal plate.

are 3 ± 0.8 dB from 28 to 32 GHz. Moreover, the isolation level between port-1 and port-4 is higher than 18 dB and the simulated phase difference between the coupled ridges is $90 \pm 2^\circ$ over the considered frequency bandwidth. To verify the results of S-parameters, Fig. 4 shows the electric field distribution of the ridge gap waveguide-based 3-dB coupler when port-1 is excited at the central frequency 30 GHz.

B. RIDGE GAP WAVEGUIDE-BASED SIX-PORT JUNCTION

As illustrated in Fig. 5, a six-port junction is a coupler structure with two input ports and four output ports. If a signal is applied on an input port (#1 or #2), the power is equally divided among the four output ports (#3, #4, #5 and #6) and consequently $|S_{31}| = |S_{41}| = |S_{51}| = |S_{61}| =$

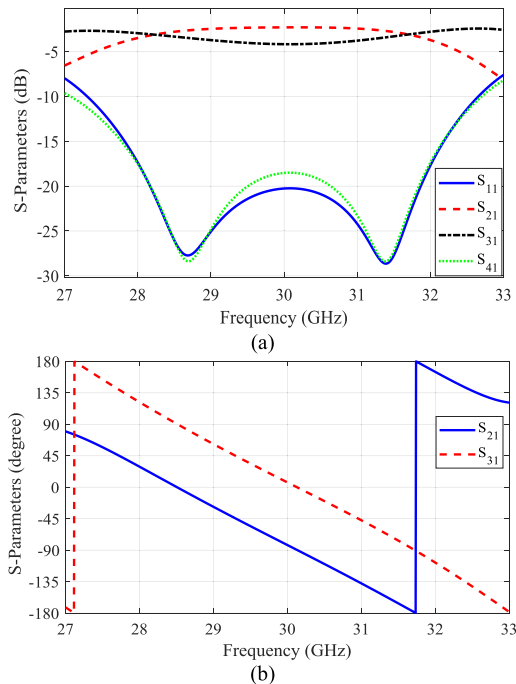


FIGURE 3. Simulated S-parameters of ridge gap waveguide-based 3-dB directional coupler.

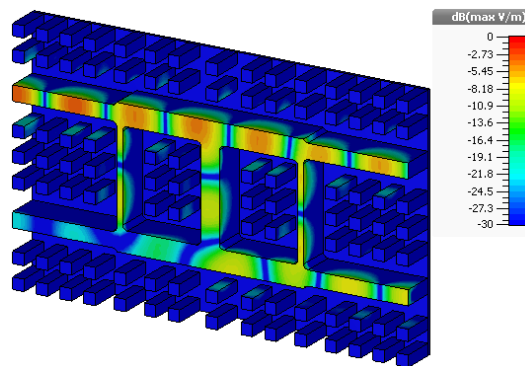


FIGURE 4. Electric field distribution of ridge gap waveguide-based 3-dB directional coupler at 30 GHz.

$|S_{32}| = |S_{42}| = |S_{52}| = |S_{62}| = -6$ dB. Moreover, in an ideal six-port junction, phase difference of output ports is 90° : $|\text{phase}(S_{31}) - \text{phase}(S_{41})| = |\text{phase}(S_{61}) - \text{phase}(S_{51})| = |\text{phase}(S_{32}) - \text{phase}(S_{42})| = |\text{phase}(S_{62}) - \text{phase}(S_{52})| = 90^\circ$. The scattering matrix for an ideal six-port junction has the following form:

$$[S] = \frac{1}{2} \begin{bmatrix} 0 & 0 & j & -1 & -1 & j \\ 0 & 0 & j & 1 & 1 & j \\ j & j & 0 & 0 & 0 & 0 \\ -1 & 1 & 0 & 0 & 0 & 0 \\ -1 & 1 & 0 & 0 & 0 & 0 \\ j & j & 0 & 0 & 0 & 0 \end{bmatrix} \quad (2)$$

Fig. 6 shows the presented six-port junction. The structure consists of three cascaded three four-port 3-dB directional

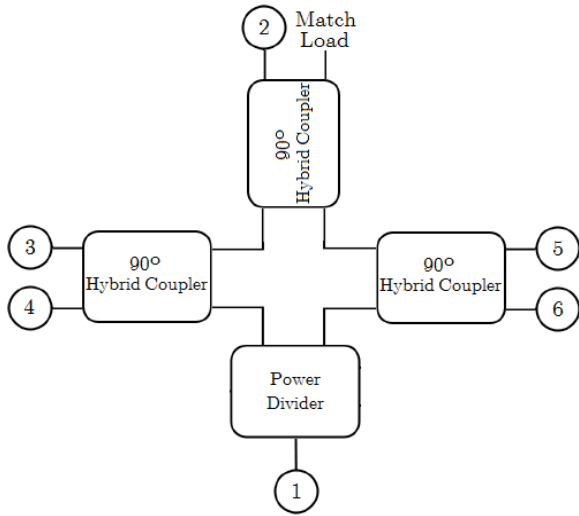


FIGURE 5. The block diagram of six-port junction.

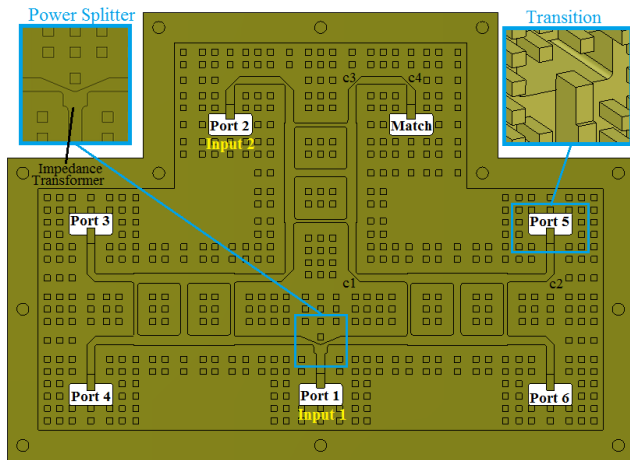


FIGURE 6. The configuration of ridge gap waveguide-based six-port junction without top metal plate.

couplers, interconnecting ridge lines and a T-junction power splitter based on gap waveguide technology to achieve good performance over the Ka band frequency range. A standard waveguide match load is employed to match the seventh port. Creating 90° bends in interconnecting ridge gap waveguides will cause a significant reflection towards the input port and only negligible part of the signal transmitted on around the bend. To overcome this challenge, chamfered bends are employed in the structure. The chamfer values (c_1 , c_2 , c_3 and c_4 shown in Fig. 6) are the amount of the outside corners of ridges that are to be sliced off and these parameters impact the input matching of the structure. Moreover, to implement the designed six-port junction, we need to a T-junction as 2-way power divider. As shown in Fig. 6, a quarter-wavelength matching section is used to achieve a wide bandwidth power divider. In addition, without V-shaped section in this power divider, it has high return loss due to the reflection of the input. The width and length of impedance

TABLE 1. Optimized design parameters of the proposed six-port junction.

Section	Parameter	Value (mm)		
		Port 1	Port 2	Port 3
Transitions	Length of Ridge	0.69	0.95	1.1
	Length of Step	2.29	2.47	2.61
	Height of Step	0.75	0.67	0.39
Power Splitter	Bases Lengths of V-shaped junction	0.14, 3.25		
	length and width of $\lambda/4$ matching section	1.39, 2.25		
Chamfer Values	$c_1 = 1.98, c_2 = 1.36, c_3 = 2.30, c_4 = 2.27$			
3-dB couplers	$w_0 = 1.30, w_1 = 0.58, w_2 = 1.70, w_3 = 1.2, l_1 = 6.96, l_2 = 8.48$ (shown in Fig. 2)			

matching section and the lengths of the bases in V-shaped junction greatly affect the input return loss of power divider.

To make the six-port junction excitable and measurable by standard flange waveguides at 30 GHz frequency band, it is required to design suitable transitions between the ridge gap waveguide and standard Ka-band waveguide (WR-28) at the input and output ports. To do this, a metal brick section with a step extending to the waveguide opening are located on the bottom wall of the structure and this is the key part of designed transition between ridge gap waveguide and WR-28 ($7.11 \times 3.56 \text{ mm}^2$). To obtain desired matching, the geometrical parameters of the metal brick should be optimized. After optimization in CST, the ultimate optimized values of the geometrical parameters of the six-port junction are tabulated in Table 1.

The simulated S-parameters of proposed six-port junction are plotted in Fig. 7. When the input port 1 is excited, the reflection coefficient is less than -20 dB and the isolation between ports 1 and 2 is higher than 20 dB over the frequency range of 28-32 GHz. Also, the amplitude and phase imbalances of the output ports of six-port junction are around $\pm 1 \text{ dB}$ and $\pm 0.5^\circ$, respectively. Similarly, according to the simulation results, the reflection coefficient of port 2 is below -17 dB and the isolation level between this port and port 2 is higher than 20 dB from 28 to 32 GHz. Also, the simulated transmission coefficients of input port 2 to the outputs ports are $-6.2 \pm 1.2 \text{ dB}$ over operating frequencies. It can be seen that the phase differences of transmission coefficients in ports 3, 4 and 5 are between $90 \pm 2.5^\circ$. For the proof of S-parameters results, the electric field distribution of the six-port junction at the central frequency 30 GHz is demonstrated in Fig. 8.

IV. FABRICATION AND MEASUREMENT

To confirm the simulation results, a prototype of six-port junction is machined using CNC milling equipment in aluminum material (with electric conductivity $3.6 \times 10^7 \text{ S/m}$). The photograph of disassembled six-port junction is illustrated in Fig. 9. The S-parameters of the fabricated prototype are measured by an Agilent network analyzer 8722ES and are shown in Fig. 10. The measured reflection coefficient of ports 1 and 2 are lower than -15 dB over the frequency range of 27.7-32.2 GHz. There exists higher than 15 dB isolation

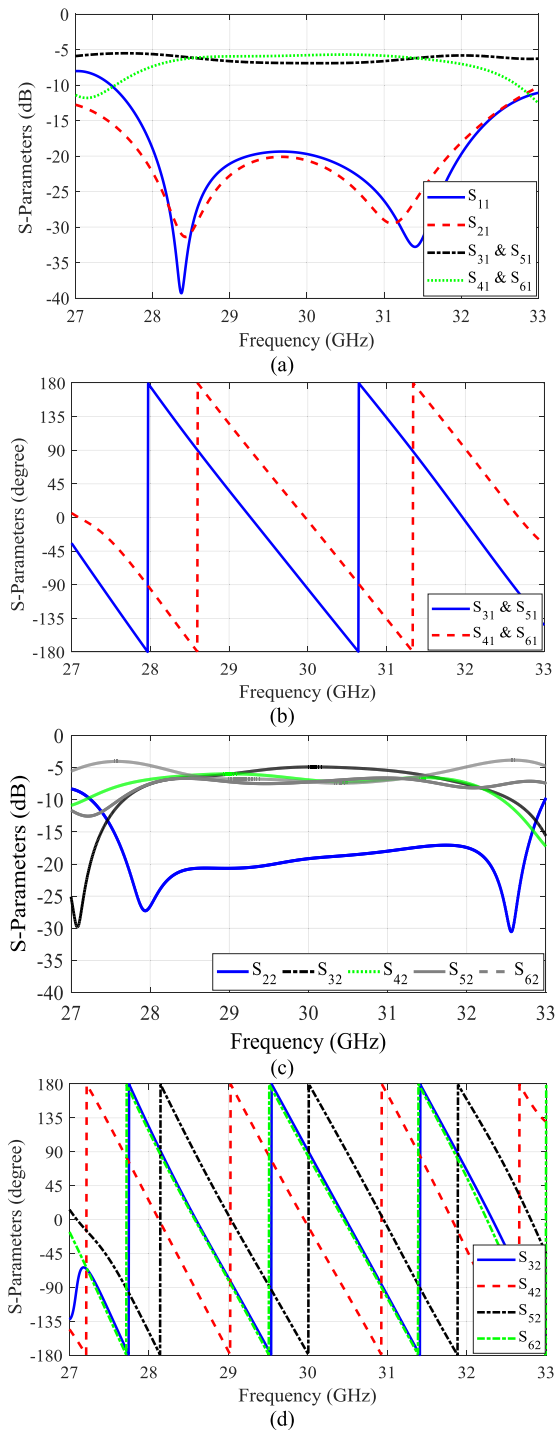


FIGURE 7. Simulated performance of proposed six-port junction. (a) Amplitudes and (b) phases of the S-parameters by exciting port 1. (c) Amplitudes and (d) phases of the S-parameters by exciting port 2.

between the two input ports in this frequency band. Also, the amplitude imbalance of the output ports of structure is around ± 1.68 dB, respectively. The slight difference between the measurement and simulation values can be attributed to the fabrication tolerance errors and alignment errors between the metal blocks.

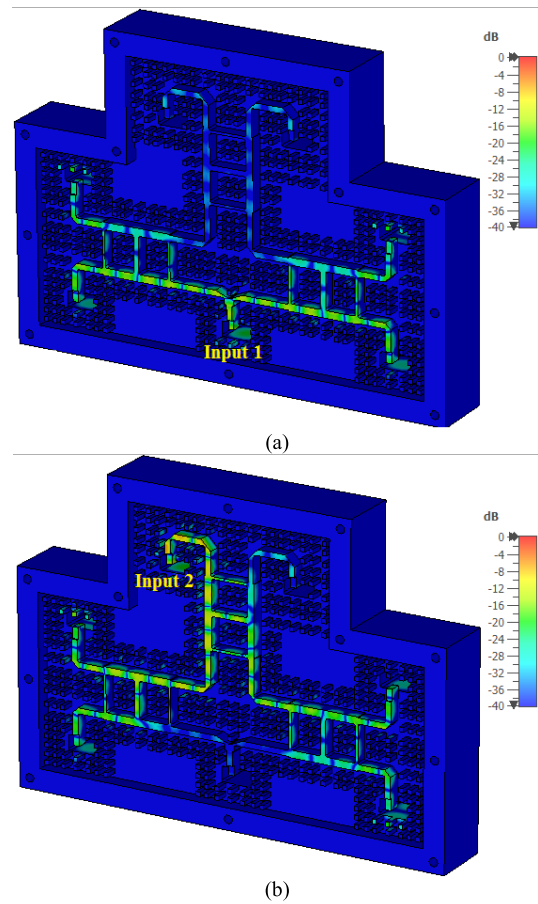


FIGURE 8. Electric field distribution of the six-port junction at the central frequency 30 GHz.

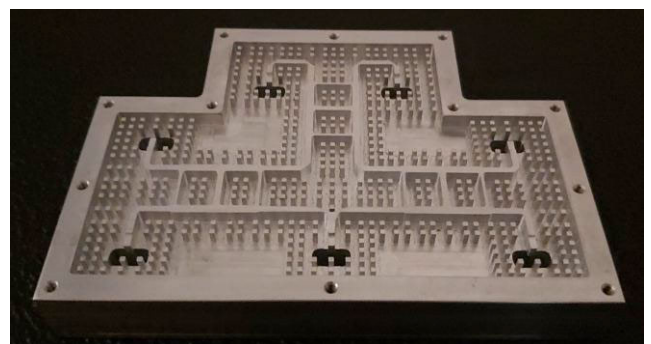


FIGURE 9. Photograph of the fabricated ridge gap waveguide-based six-port junction.

To evaluate the proposed design, the performances of various kinds of six-port junctions are compared with the present work in Table 2. The proposed structure exhibit acceptable impedance bandwidth (15%), return loss (>15 dB) and isolation levels (>15 dB) compared to other reported six-port junctions. The input bandwidth of proposed structure is higher than rectangular waveguide-based six-port junctions [14], [15], [16], [17], [18]. The amplitude imbalance and phase variation characteristics are

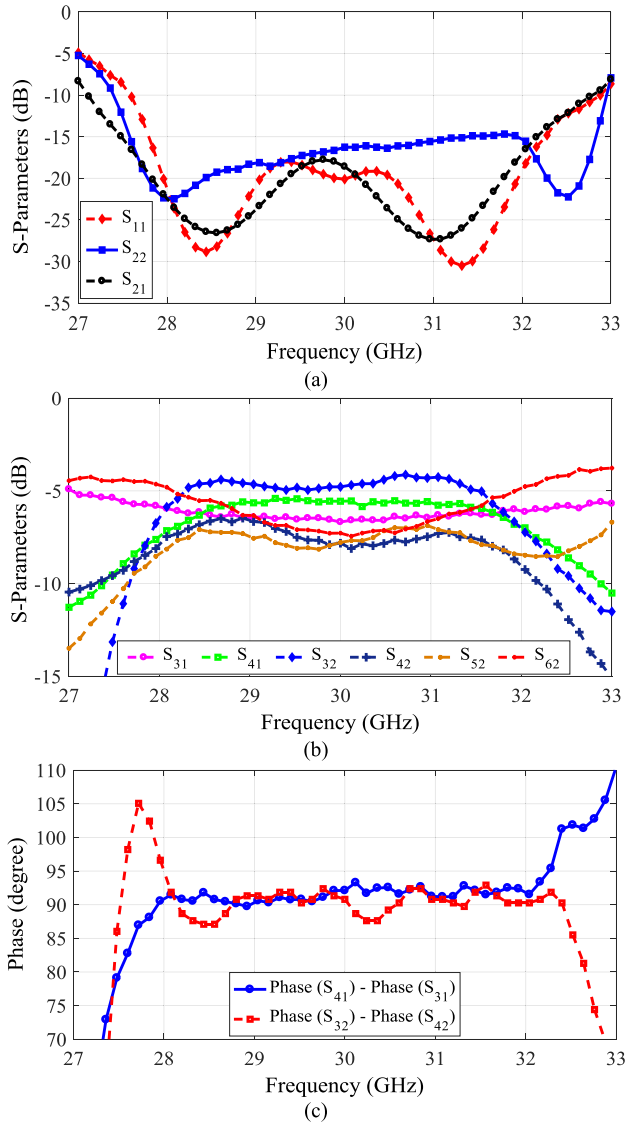


FIGURE 10. Measured S-parameters of fabricated six-port junction.

less than ± 1.68 dB and $\pm 2.5^\circ$ which is a better performance than almost all the reported six-port junctions in the table. Although the bandwidth and isolation of some SIW-based structures are better than the proposed six-port junction, it should be noted the power handling capacity of SIW-based [8], [9], [10], [11], [12] and printed ridge gap waveguide six-port junctions [28] is lower than proposed ridge gap waveguide-based structure due to the use of dielectric substrate. In addition, compared to PCB-based and SIW structures, which are lossy and low power, the dielectric and ohmic losses of the proposed junction is relatively low. By employing gap waveguide technology, providing acceptable electrical contact between the layers without using a high temperature and pressure process is performed, the manufacturing and assembly process will be simple and non-expensive. Due to the significant benefits of gap waveguide

TABLE 2. Comparison with other existing six-port junctions.

Ref.	Technology	Freq. (GHz)	B.W (%)	R. L. (dB)	Iso. (dB)	Mag. Var. (dB)	Ph. Var. (°)
[7]	Microstrip	10	10	15	20	-7.5±2.5	90±6
[8]	SIW	30.5	9.8	18	27	-8.6±0.5	90±2
[9]	SIW	12.5	10	19	20	-7.3±0.5	-
[10]	SIW	8.5	35	15	15	-7.5±1.5	88±11
[11]	SIW	13.5	22.3	17	18	-7.8±1.5	88.5±3.5
[12]	SIW	25	28	15	20	-7.4±1.5	88.5±12
[14]	Rectangular Waveguide	19	8.4	20	20	-4.9±0.15	-
[15]	Rectangular Waveguide	19	4.7	25	25	-4.75±0.75	-
[16]	Rectangular Waveguide	30	6.7	15	15	-6.4±2.1	91.5±13.5
[17]	Rectangular Waveguide	9.95	4.02	15	-	-7.4±0.5	90±5
[18]	Rectangular Waveguide	150	2.67	11	17.9	-6±0.5	90±3.2
[28]	Printed Gap Waveguide	40	10	10	15	-7±2.2	90±5
This Work	Ridge Gap Waveguide	29.95	15	15	15	-6.1±1.68	90±2.5

technology, the presented six-port junction could be a proper candidate for various mmWave applications.

V. CONCLUSION

Ridge gap waveguide technology is utilized for designing a wideband six-port junction for Ka-band applications. Using gap waveguide technology allows designing the mmWave six-port junction and coupler without the strict electrical connection requirement between various waveguide layers and metal blocks. A prototype of six-port junction is then fabricated and measured. The measured reflection coefficients of input ports and isolation level between them are better than -15 dB and 15 dB, respectively, at the center frequency of 29.95 GHz. Also, the amplitude imbalance and phase variation characteristics are less than ± 1.68 dB and $\pm 2.5^\circ$, respectively. The proposed six-port junction can be used in various broadband applications at mmWave.

REFERENCES

- [1] S. K. Yong and C.-C. Chong, "An overview of multigigabit wireless through millimeter wave technology: Potentials and technical challenges," *EURASIP J. Wireless Commun. Netw.*, vol. 2007, no. 1, Dec. 2006, Art. no. 078907.
- [2] S. O. Tatu, E. Moldovan, K. Wu, and R. G. Bosisio, "A new direct millimeter-wave six-port receiver," *IEEE Trans. Microw. Theory Techn.*, vol. 49, no. 12, pp. 2517–2522, Dec. 2001.
- [3] D. Ghosh and G. Kumar, "Six-port reflectometer using edge-coupled microstrip couplers," *IEEE Microw. Wireless Compon. Lett.*, vol. 27, no. 3, pp. 245–247, Mar. 2017.
- [4] K. Staszek, "Six-port calibration utilizing matched load and unknown calibration loads," *IEEE Trans. Microw. Theory Techn.*, vol. 66, no. 10, pp. 4617–4626, Oct. 2018.
- [5] E. Moldovan, S. O. Tatu, T. Gaman, K. Wu, and R. G. Bosisio, "A new 94-GHz six-port collision-avoidance radar sensor," *IEEE Trans. Microw. Theory Techn.*, vol. 52, no. 3, pp. 751–759, Mar. 2004.

- [6] X. Xu, R. G. Bosisio, and K. Wu, "A new six-port junction based on substrate integrated waveguide technology," *IEEE Trans. Microw. Theory Techn.*, vol. 53, no. 7, pp. 2267–2272, Jul. 2005.
- [7] H. Song, S.-B. Liu, and S. Liu, "A new six-port junction based on microstrip technology," in *Proc. 3rd IEEE Int. Symp. Microw., Antenna, Propag. EMC Technol. Wireless Commun.*, Oct. 2009, pp. 584–587.
- [8] J. Chen, W. Hong, H. Tang, P. Yan, B. Liu, and K. Wu, "A millimeter wave six-port network using half-mode substrate integrated waveguide," *J. Infr., Millim., Terahertz Waves*, vol. 33, no. 3, pp. 348–356, Mar. 2012.
- [9] M. Salehi, J. Bornemann, and E. Mehrshahi, "Wideband substrate-integrated waveguide six-port power divider/combiner," *Microw. Opt. Technol. Lett.*, vol. 55, no. 12, pp. 2984–2986, Dec. 2013.
- [10] S. Liu and F. Xu, "Novel substrate-integrated waveguide phase shifter and its application to six-port junction," *IEEE Trans. Microw. Theory Techn.*, vol. 67, no. 10, pp. 4167–4174, Oct. 2019.
- [11] X. Hu and F. Xu, "A six-port network based on substrate integrated waveguide coupler with metal strips," *IET Microw., Antennas Propag.*, vol. 16, no. 1, pp. 18–28, Jan. 2022.
- [12] B. Tegowski and A. Koelpin, "A compact stacked SIW six-port junction," *IEEE Microw. Wireless Technol. Lett.*, vol. 33, no. 5, pp. 515–518, May 2023.
- [13] E. Kuhn, H. Schmiedel, and R. Waugh, "Six-port branch-waveguide directional couplers," in *Proc. 16th Eur. Microw. Conf.*, Oct. 1986, pp. 453–458.
- [14] F. Alessandri, M. Giordano, M. Guglielmi, G. Martirano, and F. Vitulli, "A new multiple-tuned six-port riblet-type directional coupler in rectangular waveguide," *IEEE Trans. Microw. Theory Techn.*, vol. 51, no. 5, pp. 1441–1448, May 2003.
- [15] L. Zappelli, "Optimization procedure of four-port and six-port directional couplers based on polygon equivalent circuit," *IEEE Trans. Microw. Theory Techn.*, vol. 66, no. 10, pp. 4471–4481, Oct. 2018.
- [16] A. A. Sakr, W. M. Dyab, and K. Wu, "A dually polarized six-port junction based on polarization-selective coupling for polarization-inclusive remote sensing," *IEEE Trans. Microw. Theory Techn.*, vol. 66, no. 8, pp. 3817–3827, Aug. 2018.
- [17] X. Chen, Y. Wang, T. Skaik, and Q. Zhang, "E-plane waveguide filtering six-port junction," *IEEE Trans. Microw. Theory Techn.*, vol. 69, no. 12, pp. 5360–5370, Dec. 2021.
- [18] X. Chen, M. Salek, Q. Zhang, and Y. Wang, "Subterahertz filtering six-port junction," *IEEE Trans. Microw. Theory Techn.*, vol. 70, no. 8, pp. 3877–3885, Aug. 2022.
- [19] A. U. Zaman and P.-S. Kildal, "GAP waveguides," in *Handbook of Antenna Technologies*. Singapore: Springer, 2016.
- [20] J. Cao, H. Wang, S. Tao, S. Mou, and Y. Guo, "Highly integrated beam scanning groove gap waveguide leaky wave antenna array," *IEEE Trans. Antennas Propag.*, vol. 69, no. 8, pp. 5112–5117, Aug. 2021.
- [21] S. Farjana, M. Ghaderi, A. U. Zaman, S. Rahiminejad, T. Eriksson, J. Hansson, Y. Li, T. Emanuelsson, S. Haasl, P. Lundgren, and P. Enoksson, "Realizing a 140 GHz gap waveguide-based array antenna by low-cost injection molding and micromachining," *J. Infr., Millim., Terahertz Waves*, vol. 42, no. 8, pp. 893–914, Sep. 2021.
- [22] Q. Ren, A. U. Zaman, and J. Yang, "Dual-circularly polarized array antenna based on gap waveguide utilizing double-grooved circular waveguide polarizer," *IEEE Trans. Antennas Propag.*, vol. 70, no. 11, pp. 10436–10444, Nov. 2022.
- [23] D. Zarifi, A. Farahbakhsh, and A. U. Zaman, "Design and fabrication of wideband millimeter-wave directional couplers with different coupling factors based on gap waveguide technology," *IEEE Access*, vol. 7, pp. 88822–88829, 2019.
- [24] Z. Zhao and T. A. Denidni, "Millimeter-wave printed-RGW hybrid coupler with symmetrical square feed," *IEEE Microw. Wireless Compon. Lett.*, vol. 30, no. 2, pp. 156–159, Feb. 2020.
- [25] S. Peng, Y. Pu, Z. Wu, and Y. Luo, "High-isolation power divider based on ridge gap waveguide for broadband millimeter-wave applications," *IEEE Trans. Microw. Theory Techn.*, vol. 70, no. 6, pp. 3029–3039, Jun. 2022.
- [26] A. Farahbakhsh, "Ka-band coplanar magic-T based on gap waveguide technology," *IEEE Microw. Wireless Compon. Lett.*, vol. 30, no. 9, pp. 853–856, Sep. 2020.
- [27] H. Abdollahy, A. Farahbakhsh, and M. H. Ostovarzadeh, "Mechanical reconfigurable phase shifter based on gap waveguide technology," *AEU Int. J. Electron. Commun.*, vol. 132, Apr. 2021, Art. no. 153655.
- [28] X. Jiang, Y. Shi, F. Jia, W. Feng, T. Yin, J. Yu, and X. Wang, "Millimeter-wave double ridge gap waveguide six-port network based on multi-wave mushroom," *IEEE Trans. Plasma Sci.*, vol. 49, no. 12, pp. 3778–3785, Dec. 2021.
- [29] U. Nandi, A. U. Zaman, A. Vosoogh, and J. Yang, "Novel millimeter wave transition from microstrip line to groove gap waveguide for MMIC packaging and antenna integration," *IEEE Microw. Wireless Compon. Lett.*, vol. 27, no. 8, pp. 691–693, Aug. 2017.
- [30] Q. Ren, A. U. Zaman, J. Yang, V. Vassilev, and C. Bencivenni, "Novel integration techniques for gap waveguides and MMICs suitable for multilayer waveguide applications," *IEEE Trans. Microw. Theory Techn.*, vol. 70, no. 9, pp. 4120–4128, Sep. 2022.



DAVOUD ZARIFI was born in Kashan, Iran, in 1987. He received the B.S. degree in electrical engineering from the University of Kashan, Kashan, in 2009, and the M.S. and Ph.D. degrees in electrical engineering from the Iran University of Science and Technology (IUST), Tehran, Iran, in 2011 and 2015, respectively. Currently, he is an Associate Professor with the School of Electrical and Computer Engineering, University of Kashan. His current research interests include the applications of metamaterials, microwave passive components, slot array antennas, and gap waveguide technology.



ALI FARAHBAKSH was born in Kerman, Iran, in 1984. He received the Ph.D. degree in electrical engineering from the Iran University of Science and Technology, Tehran, Iran, in 2016. He is currently an Assistant Professor with the Department of Electrical and Computer Engineering, Graduate University of Advanced Technology, Kerman. His current research interests include microwave and antenna engineering, including gap waveguide technology, millimeter-wave high-gain array antenna, microwave devices, electromagnetic wave propagation and scattering, inverse problems in electromagnetic, and anechoic chamber design.



ASHRAF UZ ZAMAN (Senior Member, IEEE) was born in Chittagong, Bangladesh. He received the B.Sc. degree in electrical and electronics engineering from the Chittagong University of Engineering and Technology, Chittagong, in 2001, and the M.Sc. and Ph.D. degrees from the Chalmers University of Technology, Gothenburg, Sweden, in 2007 and 2013, respectively. He is currently an Associate Professor with the Communication and Antenna Systems Division, Chalmers University of Technology. His current research interests include high-gain millimeter-wave planar antennas, gap waveguide technology, frequency-selective surfaces, microwave passive components, RF packaging techniques, and low-loss integration of MMICs with the antennas.

...